COMPUTER SOCIETY PRESS REPRINT

REGION GROUPING FROM A RANGE IMAGE

Joon H. Han
Richard A. Volz

Dear Professor Volz,

As one of your Ph.D students, it is my great honor to dedicate our paper to you. I am very grateful to you for what you have done for me while I was a student in Michigan.

My best wishes are with you and Mary!

Joon Hee Han
Department of Computer Science,
Pohang University of Science and Technology, Korea

Reprinted from PROCEEDINGS OF COMPUTER VISION AND PATTERN RECOGNITION, Ann Arbor, MI, June 5-9, 1988

The Computer Society of the IEEE
1730 Massachusetts Avenue NW
Washington, DC 20036-1903

Washington • Los Alamitos • Brussels

THE INSTITUTE OF ELECTRICAL AND ELECTRONICS ENGINEERS, INC.

IEEE

IEEE COMPUTER SOCIETY PRESS

REGION GROUPING FROM A RANGE IMAGE*

Joon H. Han and Richard A. Volz

Robotics Research Laboratory
Department of Electrical Engineering and Computer Science
The University of Michigan, Ann Arbor, MI 48109

Abstract

This paper presents a new method of grouping range image regions such that each group of regions represents a meaningful part of an object. The set of regions, defined as *Convex Region Set*(CRS), is made by analyzing the boundary types between a pair of regions. The boundary types are classified as *convex, concave,* and *jump boundaries*. If two regions share a *convex boundary* it is assumed that they are inseparable regions, thus describing the same part(object). The CRSs are determined by a *Region Boundary Graph*(RBG) which is defined as a graph whose nodes represent regions, and the edges represent boundaries: convex and concave. Since jump boundaries represent no physical contact in 3-D, they are represented as null edges. A CRS is defined as set of regions(or nodes in an RBG) such that for each pair of regions in the set, there is a path, which is represented only by *convex* edges. The physical interpretation is that a CRS represents part of an object such that the regions in the set can not be separated.

1 Introduction

This paper describes a new way of analyzing segmented range images to recognize 3-D objects, and follows earlier work by Han, *et al.*[7] on range image segmentation using surface normal analysis. The basic philosophy of our method is to use the nature of the range data and 3-D objects in studying the relationships between segmented range images, and to make sets of regions that partition the image regions in such a way that the regions in a set are inseparable from each other, and represent a meaningful part of a 3-D object. As an analogy with a sheet of paper, we are trying to use two faces of a sheet as one unit in matching, instead of dealing with two faces separately. The aim of this scheme is to remove non-candidate regions (or models) in the earlier stage of data driven matching by testing simple binary relationships without expansive computations, like geometric transformations or optimization.

The reduction of computation for matching comes from several factors. One factor is that the number of candidates is greatly reduced since a set of regions is a matching unit. Another factor is that, since one set of regions can be a unique combination(or at least very small number of candidate groups might exist), detection of a unique set of regions saves unnecessary searching. Additional speed up comes from the fact that only binary relationships need to be tested in the earlier stage of matching which is relatively simple. And, this method also could be a preprocessor for the matching method described by Shapiro, *et al.*[13] who used parts in matching 3-D objects using relational paradigm.

In matching geometric descriptions for range image analysis, researchers used optimization [1], relaxation[3], various tree search methods[5,9,10,12] and so forth. None of these methods used a group of regions as a unit, even though some of them used relational constraints. Depending upon the image and the models, the number comparisons or calculations in finding correspondence could be enormous in matching by one primitive to one primitive.

Some analogous but quite different work has been done in understanding 2-D line drawing of 3-D blocks world. According to Ballard and Brown[2], Guzman[6] used lines to make polygonal regions and grouped the regions such that each of the set represents one polyhedral block.

As another interpretation of line drawing of 3-D blocks world, Clowes[4] used line labeling schemes. Similar works on interpretation of line drawings can be found in Winston[15, 16]. Sugihara [14] also used junction types in analyzing 3-D block objects from range images.

The region grouping method described in this paper is based on the boundary types between two segmented regions of range image. The boundary types are *jump, convex,* and *concave*. If two regions are combined by a convex boundary, it is assumed that the two regions belong to the same object, and they are *non-separable* regions. One assumption is that we exclude accidental alignment which can be resolved through model driven analysis.

In the next section, an overview of the segmentation method is presented. Boundary types are defined in Section 3. In Section 4, CRS is defined, and in Section 5, experimental results are given, followed by a summary.

*This work was supported by the Army Research Office under grant no. DOD-C-DAAG29-84-K-0070.

2 Segmentation

In this section we summarize our segmentation procedure. A more detailed description can be found in Han, *et al.* [7,8].

The method is to find specified surfaces like, planar, cylindrical, and spherical regions that are the majority of man-made parts. After calculating surface normals using a normal operator, each type of the region is extracted in sequence. The basic strategy of this segmentation is to use maximum possible curved regions in order to capture curved surfaces, while restricting the application to a region enclosed by jump boundaries and other extracted regions in order to maintain homogeneity of the region.

Planar regions are extracted by making normal histograms and extracting regions of corresponding sizable height of the smoothed normal histograms, flowed by *planarity test* which compares the estimated overall normal of the region to the normals of inside, and outside of the boundary of the region. Without this planarity test, it is not possible to distinguish small part of slightly curved surfaces with planar regions.

Cylindrical regions are extracted by first estimating the possible direction of axis. The direction of axis is estimated using histogram analysis of cross product of a pair of normals. Then a rotation matrix is made, and surface points are projected to a plane perpendicular to the axis of the cylinder. From this projection, center point and radius, and concavity-convexity of the cylindrical regions is determined.

Spherical region extraction is based on the evidence of the center of a sphere which is made by estimating possible center points for each pair of surface points, and deciding the majority value of the center. The radius is determined from this estimated center at the same time. Distance criteria, which test the distance from surface point to the estimated center, is applied to remove false center points.

3 Boundary Types

In most cases, the properties of a region are not specific enough to find a unique candidate region in matching. There may be several candidate regions for a region of an image with the same region properties. To reduce this ambiguity, not only the property of a region but also relationships between regions must be checked. Two *binary relationships* are defined between a pair of regions such that different viewing position does not affect their relationships. The first is a *boundary type relationship* defined between two adjacent regions; the other is *region relationship value* that is measured quantitatively such as inner product of surface normals in *planar–planar* relationships, and the shortest distance from a plane to the center of a sphere in *planar–spherical* relationships and so forth. The region relationship value is useful in checking consistency between matched regions, but in this paper we only introduce the *boundary type relationships*. Winnowing, and matching sets of regions using region properties and these binary relationships are described in Han[8].

Three boundary types are defined between two adjacent regions. They are *jump boundary*, *concave boundary*, and *convex boundary*. As shown in Figure 1, for each boundary point b_i, we define a pair of points (p_i, q_i) such that $p_i \in R$, $q_i \notin R$, and the line connecting p_i and q_i meets perpendicular to the tangential line of boundary curve at b_i, and the distance from b_i to q_i is the same as that from b_i to p_i. As the distance between b_i and q_i, *chessboard distance* of 4 pixels is used. But in calculation, there are cases that the distances can not be made the same since the region could be an arbitrary shape. In this case the distance could be different, but the point p_i should be in the region, and q_i should be kept outside of the region.

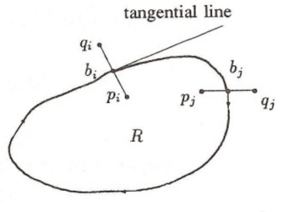

Figure 1: Boundary points, and inner and outer points.

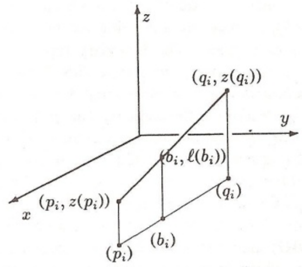

Figure 2: Relations between b_i and $\ell(b_i)$

• *Jump boundaries* : A boundary point b_i is a *jump boundary point* if $|z(p_i) - z(q_i)| > DEPTH_{THRESH}$, where $z(p_i)$ represents the depth value at point p_i, $z(q_i)$ represents depth value at point q_i, and $DEPTH_{THRESH}$ represents a threshold value of the depth difference. A *jump boundary* consists of *jump boundary points*. That is, if two regions share a boundary whose boundary points are jump boundary points, then the boundary is a jump boundary. In a range image two neighboring regions can share a jump boundary, but in actual

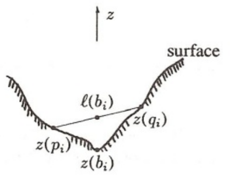

Figure 3: Concave boundary point.

3-D, they are not neighbors. Hence, if two adjacent regions share a jump boundary in range image, we declare them as *non*-neighbors.

Let $b_i = (b_{ix}, b_{iy})$ be a boundary point. Let ℓ be a line in 3-D space that passes through $(p_i, z(p_i)) = (p_{ix}, p_{iy}, z(p_i))$ and $(q_i, z(q_i)) = (q_{ix}, q_{iy}, z(q_i))$. We use the notation $\ell(b_i)$ to denote the z-coordinate value of the line at point (b_i), that is, the point on the line ℓ is $(b_i, \ell(b_i)) = (b_{ix}, b_{iy}, \ell(b_{ix}, b_{iy}))$ and the depth value of the range image at point b_i is denoted as $z(b_i)$(see Figure 2).

• *Concave Boundary* : A boundary point b_i is a *concave boundary point* if $\ell(b_i) > z(b_i)$. That is, the depth value of the boundary points is below the line segments that connects point p_i and q_i as shown in Figure 3. In the figure, the cross section is shown with vertical axis representing the depth value of the surfaces. A boundary is a *concave boundary* if its boundary points are *concave boundary points*.

• *Convex Boundary* : A boundary point b_i is a *convex boundary point* if $\ell(b_i) \leq z(b_i)$. Actually, if $\ell(b_i) = z(b_i)$ then b_i is neither convex nor concave. But in this case we define it as a convex point as explained later. A boundary is a *convex boundary* if its boundary points are convex boundary points.

As an example of the boundary types, let's consider Figure 4 as a segmented range image of a cylindrical block on a floor with a wall. In the figure, the boundary types between regions 1 and 2, and 1 and 3 are jump, between regions 1 and 4, and 3 and 4, are concave. The boundary type between regions 2 and 3 is convex. As we can see from the figure, there are more than one type of boundary between regions 3 and 4. For region 3, two vertical boundaries are jump, and the bottom boundary is concave. But, since jump means no physical contact, the relation between regions 3 and 4 is defined as *concave*. As in this example, two regions may share more than one type of boundary. In this case the relation is determined by the strength of the boundary types as defined next.

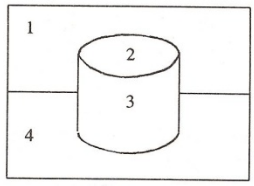

Figure 4: Region boundaries.

• *Strength of a boundary type* : The *strength of a boundary type* means *the strength of the relationship between two regions that share the boundary*. For example, the jump boundary between regions 1 and 2, in Figure 4, has no physical contact. Hence, the jump boundary is the weakest boundary type among the three. The concave boundary as between regions 3 and 4 and between regions 1 and 4, shows actual contact between those regions. This type is stronger than a jump boundary. But two regions that share a concave boundary do not necessarily belong to the same part. This boundary type can be formed when we put an object on another.

Convex boundaries, on the other hand, cannot be made this way except through an accidental alignment. If two regions share a convex boundary, as in most of the cases, they belong to the same object. That is, they cannot be separated. Hence a convex boundary is the strongest type. In other words, the strengths of the boundary types are ordered as *convex> concave> jump*. If two regions share more than one type of boundary, the relation is defined by the strongest boundary type.

• *Accidental alignment* : In defining the strength of boundary types, we excluded accidental alignment of objects. If two or more objects contact in such a way that they form a convex boundary(Figure 5-A), or two regions merge to one region(Figure 5-B), it is not possible to say whether the observed object is a single object or combination of several objects without knowledge of the models. The left side object in Figure 5-B could be a combination of two blocks as shown in the figure, or it could be a single object. Or, it could be a combination of more than two objects. In our analysis, these cases are regarded as a single object. It is assumed that this accidental alignment problem can be resolved in higher level analysis using model data.

If two regions share a boundary where $(\ell(b_i) - z(b_i))$ is positive and close to zero, then the regions are supposed to be *inseparable*. And b_i is regarded as the convex boundary point. Hence, the convex boundary point is defined as the point where $\ell(b_i) \leq z(b_i)$ instead of $\ell(b_i) < z(b_i)$.

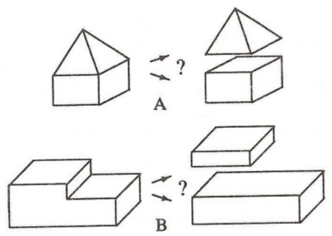

Figure 5: Accidental alignment of objects.

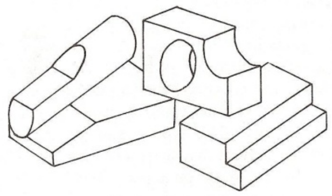

Figure 6: Region boundaries of objects.

4 Convex region set

Let's consider Figure 6 as a drawing of some objects. Humans can easily perceive this picture as a drawing of four objects jumbled together. But for machines, this picture is just a set of regions(or line segments if you will). Let's consider the same picture as region boundaries of a segmented range image. Then there are 18 regions without considering the background.

If there is a way of grouping those regions into four sets such that each set only matches one part(object), then matching will be much faster and computation will be greatly reduced compared to region by region matching. In this section we introduce *Convex Region Set(CRS)* which is a set of range image regions such that each of the regions in a set only matches one object.

We use graph notation in representing the regions and boundary relationships. Some of the definitions of graphs are given as follows. We will assume that the graph under consideration is *simple* and *undirected* .

- Any sequence of edges of a graph such that the terminal node of any edge in the sequence is the initial node of the edge, if any, appearing next in the sequence defines a *path* of the graph.

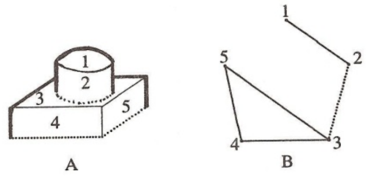

Figure 7: Segmented boundary types(A) and graph representation(B).

- A node v of a graph is said to be *reachable(accessible)* from the node u of the same graph, if there exists a path from u to v.

Let's represent region and boundary types by a graph. A region is represented by a node. Even though there are different surface(region) types, we use one type of representation as the node. A boundary between two regions is represented by an edge. A convex boundary is represented by a solid edge, a concave boundary is represented by a dotted edge, and a jump boundary is represented by a null edge, that is, there is no edge since jump boundary means no physical contact. If there are more than one type of boundary types between two regions, the strongest boundary type represents the relationship. As we mentioned earlier, convex is the strongest boundary and then concave. As an example, Figure 7-A represents segmented regions with boundaries, where dotted lines represent concave boundaries, thick lines represent jump and thin lines represent the convex boundaries. Figure 7-B represents the corresponding region boundary graph. This representation is similar to the attributed relational graph used by Kak, *et al.* [11].

Definition 1 A *Region Boundary Graph(RBG)* $G = (R, CV, CC)$ consists of a nonempty set R representing the set of regions, CV is the set of convex edges which represent convex boundaries, CC is the set of concave edges representing concave boundaries.

Definition 2 Any sequence of *convex* edges of an *RBG* such that the terminal node of any convex edge in the sequence is the initial node of the convex edge, if any, appearing next in the sequence defines *convex path* of the *RBG*.

For example, (3,5)(5,4)(4,3) and (1,2) are convex paths in Figure 7-B.

Definition 3 A node v of an *RBG* is *convex reachable* from the node u of the same *RBG* if there exists a convex path from u to v.

Definition 4 A *Convex Region Set (CRS)* S of an *RBG* is a set of regions such that any node $v \in S$ is *convex reachable* from any node $u \in S$.

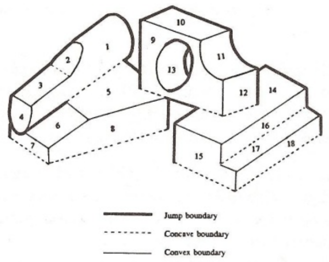

Figure 8: Region boundary representation of Figure 6.

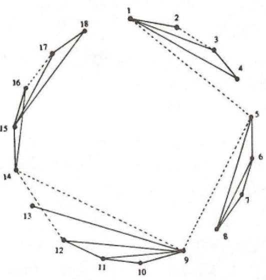

Figure 9: Region boundary graph of Figure 8.

As an example, in Figure 7-B, there are two CRSs. One is $\{1,2\}$, and the other is $\{3,4,5\}$. If we compare the regions in Figure 7-A with the CRS, a cylindrical object consists of regions 1 and 2 which are elements of CRS $\{1,2\}$, and the bottom block consists of regions 3, 4, and 5 which are the elements of CRS $\{3,4,5\}$. The relationship between regions 2 and 3 is weak and may be separated. We don't know whether the cylinder is glued to the block, or it is just on top of the block.

With this knowledge, we can regard regions 1 and 2 as one unit and regions 3, 4, and 5 as another unit in matching. Now it is clear what the physical interpretation of CRS is and why it will be useful in matching. As another example, Figure 8 represents the region boundary types of the regions shown in Figure 6. Figure 9 represents the RBG of Figure 8.

There are four CRSs in Figure 9; they are,

$$\{1,2,3,4\}, \ \{5,6,7,8\},$$
$$\{9,10,11,12,13\}, \ \text{and} \ \{14,15,16,17,18\}.$$

The regions in each set make a separate object. Notice that the CRS has no relationships with the convexity or concavity of the parts described by the CRS. It is the relationships between regions of the objects.

• *Weighting of the CRS* : In selecting the order of CRS for matching, it is better to choose a CRS that has many regions, or that has more unique regions. This can be made by giving a weighting factor to each of the regions in a CRS. Considering that planar regions are most abundant and have less features than curved regions, a weighting factor of 1 is given for each planar region. Cylindrical regions are more abundant, thus we assigned 2 for cylindrical regions and 3 for spherical regions. The total weight of a CRS is the sum of each of the region's weighting factor.

5 Computation of CRS from Range Image

In this section CRS calculation results are shown for the range images that are made synthetically using a geometric modeling system. The depth value is represented by 8 bits(0 to 255), but the parts of the objects occupy only a small range of this depth value. For example, the radii of the cylindrical regions in Figure 11 are 9, 13, and 18. Normal distribution noise with standard deviation of 2.0 is added to the image.

After segmenting the range images, CRSs are made according to the boundary relationships between pairs of regions. From the results of region segmentation, the boundary of each of the region is followed, and boundary points are classified as convex, concave or jump in relation with other regions. With this boundary point type and labels of neighboring regions, boundary types between pair of regions are decided. Boundary relationships between two regions are determined by the strongest boundary type. Two regions can be neighbors if they share non-zero number of boundary points.

The results of some of our many tests are shown here. We named the range images as Image-A, Image-B, etc. In Figure 10, (a) is the original range image, and (b) is the segmented regions. In this case there are 5 planar regions, a cylindrical region, and a spherical region connected smoothly to the cylindrical region. There are four CRSs in this segmented image. The *non-black* regions in (c), (d), (e), and (f) show each of the CRS. (e) and (f) consist of only one region for each of the CRS. Figure (g) shows the region boundaries, region labels, and location of the spherical region center(big cross line) and two end points(represented by '+') of cylindrical axis(line connecting two '+'s). Note that region labels are not necessarily in sequence. The CRS shown in (c) has the largest weighting among the CRSs, meaning the CRSs has the most informative shape. (h) is the RBG of the segmented regions, where solid lines represent convex boundaries, and dotted lines represent concave boundaries. The small black squares represent nodes which represent regions. The labels of each node consist of two parts, like, (P 1), (C 7), (S 8) etc. Here, a 'P' represents a planar region, a 'C' represents a cylindrical region, and an 'S' represents a spherical region. The numbers, 1, 7, 8 are the region labels.

In Figure 11, the object contains concave and convex cylindrical regions. In this figure also, (a) is the range image, and (b) is segmented regions. (c) shows a CRS that has a convex cylindrical region, a planar region, and a concave cylindrical region. These three regions are connected by convex links as shown in (h)(regions 3,7,8). (d) is another CRS with a convex cylinder and a plane(regions 5 and 9). The CRS shown in (e) has two planar regions(regions 4 and 6), and (f) is the background region(region 1). (g) shows the region boundaries and axes of cylindrical regions. Figures 12 and 13 show other examples.

6 Summary

A new method of grouping range image regions is presented, and computational examples are given. The group of regions, defined as a *Convex Region Set*(CRS), represents a part(or object) such that those regions in a CRS are inseparable. The CRS is made by analyzing boundary types, *convex, concave, and jump*, between a pair of regions. If two regions share a convex boundary, it is assumed that they are inseparable, and they belong to the same CRS. This method can be applied to any range image regions, convex or concave, or curved parts where boundaries are defined.

This technique is very useful in analyzing 3-D scenes using range data, and can be used as a preprocess for 3-D matching where the unit of matching is a part of an object(or set of regions) instead of one region. Thus greatly reducing the computation of matching.

High level model driven analysis will be required if some parts do not exist in model data. This could happen if two or more parts merge together and appear to be a single part.

In order to calculate the pose of object, geometric parameters(rotation and translation) must be calculated. With matched set of regions, this computation will be easy compared to conventional region to region matching. More work will be done for this transformation computation.

References

[1] N. Ayache, O. Faugeras, and B. Faverjon. " A Geometric Matcher for Recognizing and Positioning 3-D Rigid Objects". *SPIE Intelligent Robots and Computer Vision*, pp. 152–159, 1984.

[2] Dana H. Ballard and Christopher M. Brown. *Computer Vision*. Prentice-Hall, Inc., Englewood Cliffs, 1982.

[3] Bir Bhanu. "Representation and Shape Matching of 3-D Objects". *IEEE Tran. on Pattern Analysis and Machine Intelligence*, vol. PAMI-6(num. 3) pp. 340–351, May 1984.

[4] M. B. Clowes. "On seeing things". *Artificial Intelligence*, vol. 2 pp. 79–116, 1971.

[5] W. Eric L. Grimson and Tomas Lozano-Perez. "Model-Based Recognition and Localization from Sparse Range or Tactile Data". *The International Journal of Robotics Research*, vol. 3(num. 3) pp. 3–35, 1984.

[6] A. Guzman. "Decomposition of a visual scene into three-dimensional bodies". In A. Grasseli, editor, *Automatic Interpretation and Classification of Images*, Academic Press, New York, 1969.

[7] Joon H. Han, Richard A. Volz, and Trevor M. Mudge. "Range Image Segmentation and Surface Parameter Extraction for 3-D Object Recognition of Industrial Parts". *Proc. on 1987 IEEE International conf. on Robotics and Automation*, vol. 1 pp. 380–386, March 1987.

[8] Joon H. Han. "Range Image Analysis for 3-D Object Recognition". Ph.D. dissertation, EECS Dept., The University of Michigan, Ann Arbor, 1988.

[9] M. Hebert and T. Kanade. "The 3-D Profile Method for Object Recognition". *IEEE Proc. CVPR*, pp. 458–463, June 1985.

[10] Patrice Horaud and Robert C. Bolles. "3DPO's Strategy for Matching Three-Dimensional Objects in Range Data". *IEEE Computer Society Int'l Conf. on Robotics*, pp. 78–85, March 1984.

[11] A. C. Kak, A. J. Vayda, R. L. Cromwell, W. Y. Kim, and C. H. Chen "Knowledge-Based Robotics". *Proc. on 1987 IEEE International conf. on Robotics and Automation*, vol. 2 pp. 637-646, March 1987.

[12] Masaki Oshima and Yoshiaki Shirai. "Object Recognition Using Three Dimensional Information". *IEEE Trans. PAMI*, vol. PAMI-5(num. 4), July 1983.

[13] Linda G. Shapiro, John D. Moriarty, Robert M. Haralick, and Prasanna G. Mulgaonkar. "Matching Three-Dimensional Objects Using a Relational Paradigm". *Pattern Recognition*, vol. 17(num. 6) pp. 385–405, 1984.

[14] Kokichi Sugihara. "Range-Data Analysis Guided by a Junction Dictionary". *Artificial Intelligence*, vol. 12 pp. 41–69, 1979.

[15] P. H. Winston, editor. *The Psychology of Computer Vision*. McGraw-Hill, New York, 1975.

[16] Patrick Henry Winston. *Artificial Intelligence*. Addison-Wesley Publishing Company, 1979.

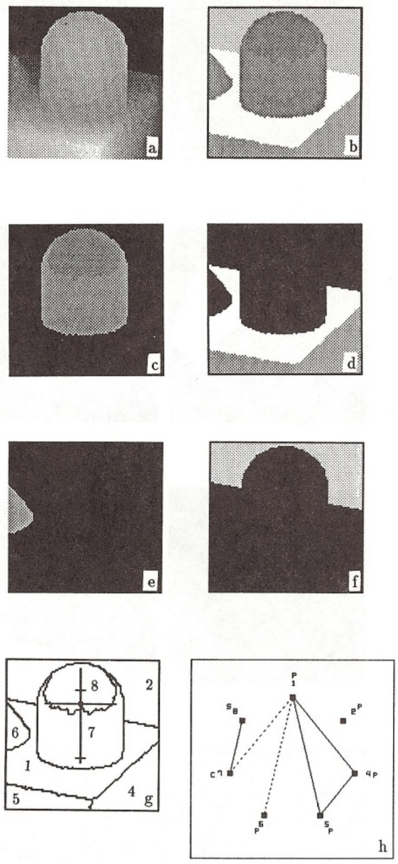

Figure 10: CRS and RBG of Image-A.

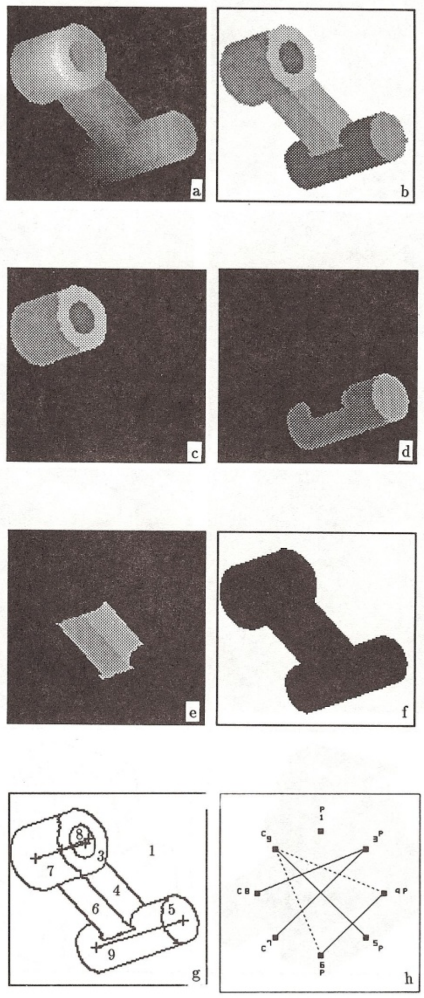

Figure 11: CRS and RBG of Image-B.

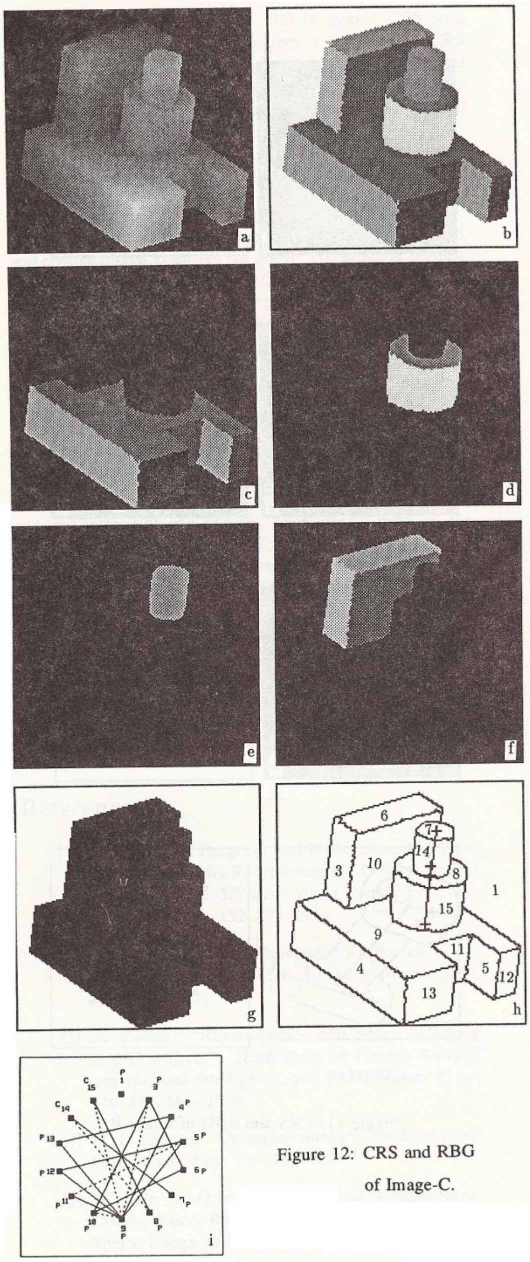

Figure 12: CRS and RBG of Image-C.

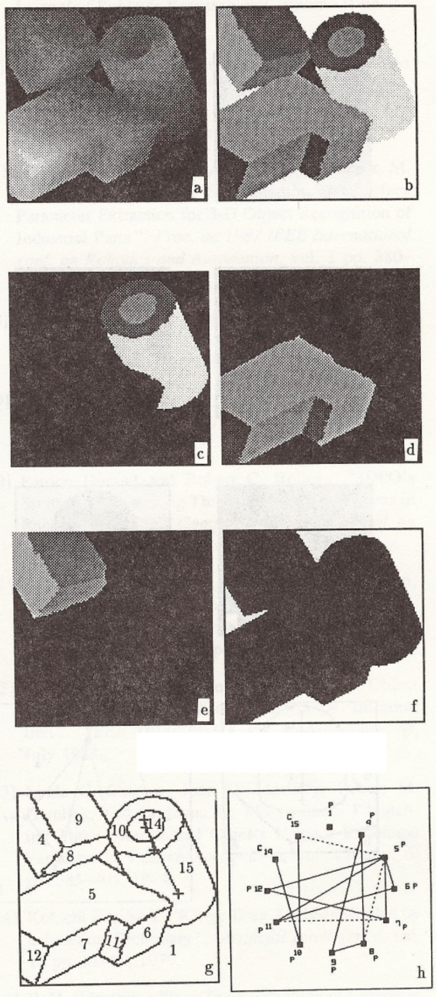

Figure 13: CRS and RBG of Image-D.